A magnetovariational study in Central Italy: Standard techniques

Emanuele Bozzo, Giorgio Caneva, Antonio Elena, Marco Gambetta and Enzo Zunino
Dipartimento di Scienze della Terra, Università di Genova, Italy

Abstract
A magnetovariational study was performed in Central Italy, with an array of magnetometers located at Radicondoli (SI), Radda in Chianti (SI), Roccalbegna (GR), Città di Castello (PG) and Pennabilli (PS) from February to May 1992. Geomagnetic transfer functions in the frequency domain were calculated using the standard least squares tecnique. The induction arrows for the periods $T = 32$ min and $T = 128$ min, the Hypothetical Event (HE) maps and two $|Z/H|$ pseudosections across the array, show the magnetovariational effect of the upper mantle anomaly in the Tuscan-Tyrrhenian area and the contrast between different crustal types.

Key words *magnetovariations – Parkinson induction arrows – pseudosections – Tuscan geothermal anomaly – Tyrrhenian upper mantle anomaly*

1. Introduction

As known, lateral anomalies of electrical conductivity in the Earth's crust and mantle can be investigated by magnetovariational techniques (geomagnetic depth soundings). Conductive bodies are interpreted in terms of geodynamic features, heat flow and lateral inhomogeneities in the crust and mantle (*e.g.* Chave and Booker, 1987; Gough, 1989; and references therein).

A magnetovariational study along a profile crossing Corsica and Sardinia has already emphasized the existence of two major conducting bodies, respectively north of Corsica and south of Sardinia. Local conductivity anomalies also exist in Northern Corsica, across the Bonifacio straits and along the Campidano Graben (Balia *et al.*, 1991; Cerv *et al.*, 1993).

This paper deals with depth geomagnetic soundings performed in Central Italy from February to May 1992, to study the electrical conductivity anomalies related to the Tuscan-Tyrrhenian upper mantle anomaly (UMA) and to the Tuscan geothermal anomaly, which are connected with the presence of a thinned lithosphere overlying a low-rigid hot mantle (Della Vedova *et al.*, 1991).

The Tuscan UMA extends eastwards from Northern Corsica, covering part of the Northern Tyrrhenian Sea and of the North-Central Apennines. The eastern border of the Tuscan upper mantle anomaly is marked by a transition from positive to negative values of the Bouguer anomalies, as well as by a strong decrease in high heat flow density (HFD) and an increase in seismicity towards the Apenninic chain. Two HFD anomalies of wide extent are located respectively over Tuscany and the Tyrrhenian sea. The latter anomaly can be due to the oceanization of the Tyrrhenian area; conversely the Tuscan anomaly, of continental nature, is ascribed to the extension processes at the western margin of the Apulian platform (*e.g.* Lavecchia, 1988; Mongelli *et al.*, 1989; Morelli and Nicolich, 1990; Della Vedova *et al.*, 1991; and references therein).

2. Magnetovariational data

Five fluxgate magnetometers with digital data acquisition systems were settled to cover the main structural features of the Tuscan upper mantle anomaly (fig. 1). The magnetovariational stations were located at Radicondoli, Radda in Chianti, Roccalbegna, Città di Castello and Pennabilli; the acronyms with geographical coordinates are listed in table I. Each magnetovariational station consisted of a three-component (X, Y, Z) fluxgate magnetometer, a datalogger based on a Z80 microprocessor and a low-power tape recorder. The time variations of the geomagnetic field were recorded with an accuracy of 0.1 nT, at a sampling rate of 60 s. The datalogger digitalization program uses an input low pass filter (2.5 min of moving average), to eliminate anthropic disturbances. Further digital filters eliminate thermal drifts. Both bay-like variations and polar disturbances are utilized in this study. These events are listed in table II.

The data are worked out by applying a cosine tapered windowing, a high pass filter (2nd degree detrend) and a residuation from the mean value. The Discrete Fourier Transform (DFT) is calculated; the data in the frequency domain are then used to calculate the Transfer Functions (TF) using the standard least squares

Table I. Acronyms and geographical coordinates of the magnetovariational stations.

Station	Acronym	Latitude	Longitude
Radicondoli	RDC	43°14′ N	11°01′ E
Radda in Chianti	RDD	43°28′	11°27′
Roccalbegna	RAB	42°47′	11°28′
Città di Castello	CDC	43°21′	12°08′
Pennabilli	PNB	43°48′	12°17′
Asco	ASC	42°25′	08°57′
Campana	CMP	42°24′	09°22′

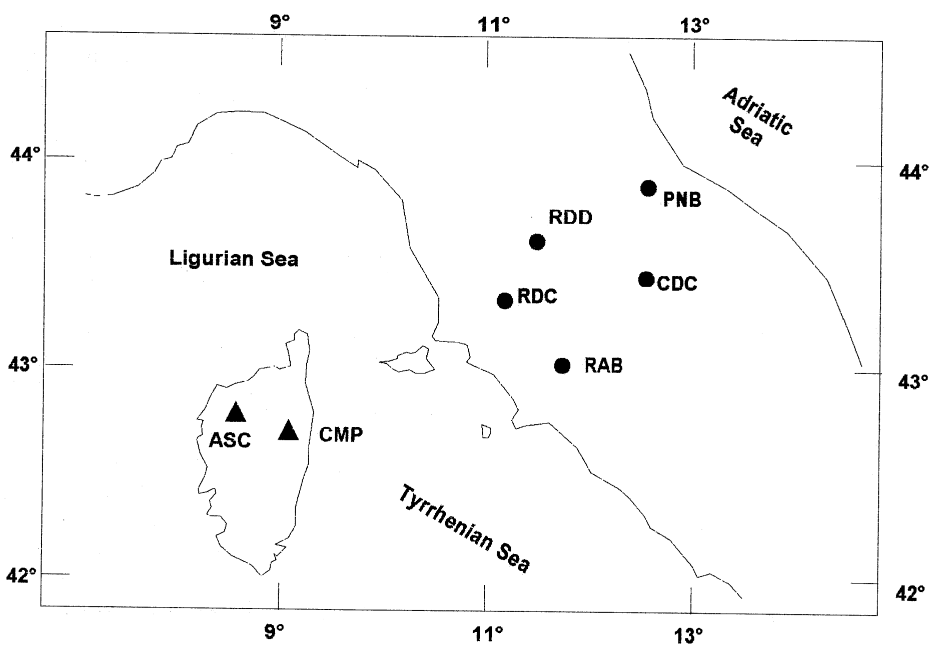

Fig. 1. Map of the magnetovariational stations utilized in this study.

Table II. List of baylike and polar substorm events utilized in this study.

Year	Month	Days
1992	February	25, 26, 27, 29
1992	March	09, 16, 17, 18, 21, 24, 26, 30, 31
1992	April	02, 03, 08, 18, 25
1992	May	01, 07, 09, 10, 18, 22, 23

techniques (see *e.g.* Everett and Hyndman, 1967).

As known, at the surface of a conductive halfspace the magnetovariational field induces currents which, by electromagnetic interaction, increase the amplitude of geomagnetic horizontal variations and decrease those of the vertical components (*e.g.* Gough and Ingham, 1983)

From an analysis of the signal in the frequency domain, some indication about the depth and thickness of the geological structure which is responsible for the anomaly, can be obtained.

Indeed, the well known relation

$$Sd = 30.2\,(T/\sigma)^{1/2} \qquad (2.1)$$

T: [h]; σ: [Siemens/m]; Sd: [km]

gives the skin depth Sd of the subsoil of conductivity σ which can be controlled by an electromagnetic signal of period T.

From the magnetovariational data in the frequency domain, the geomagnetic transfer functions $A(\omega)$ and $B(\omega)$ can be derived on the basis of the relationship

$$\Delta Z(\omega) = A(\omega)\,\Delta X(\omega) + B(\omega)\,\Delta Y(\omega) \qquad (2.2)$$

where ω is the angular frequency.

The real parts, $A_r(\omega)$ and $B_r(\omega)$, can also be graphically represented by a couple of induction arrows, whose real part (in-phase) has magnitude

$$|V_r| = (A_r^2 + B_r^2)^{1/2} \qquad (2.3)$$

pointing at angle α_r clockwise from north

$$\alpha_r = \arctan\,(B_r/A_r) \qquad (2.4)$$

and similar for the imaginary (quadrature-phase) vector.

The transfer functions can be used with the Hypothetical Event (HE) technique to map the vertical field of the currents induced by a hypothetical horizontal field, linearly polarized, of unit amplitude, as follows:

$$Z_{r,i}(\omega) = A_{r,i}(\omega)\cos\alpha + B_{r,i}(\omega)\sin\alpha \qquad (2.5)$$

where ω is the angular frequency and α the polarization azimuth.

Moreover, the anomalies of electrical conductivity can be investigated by means of the ratio $|Z|/|H|$ for a hypothetical horizontal field, as follows:

$$\rho(\omega) \propto |Z/H| \qquad (2.6)$$

The results obtained along profiles by these techniques are useful for the interpretation of conductive geostructures (*e.g.* Ingham *et al.*, 1983).

3. Results

The behaviour of horizontal components of magnetovariations at all stations in fig. 2 is similar, because of the spatial uniformity of the primary inducing field over the investigated area; conversely the vertical component shows significant differences between stations RAB and PNB.

The representation of transfer functions with induction arrows allows a comparison between our results and other geophysical data in this area, such as HFD and gravimetric Bouguer anomalies.

At the period of 128 min (fig. 3a,b) the real arrows point towards a marked discontinuity in electrical conductivity, located in the area of maximum gradient of the heat flow density and

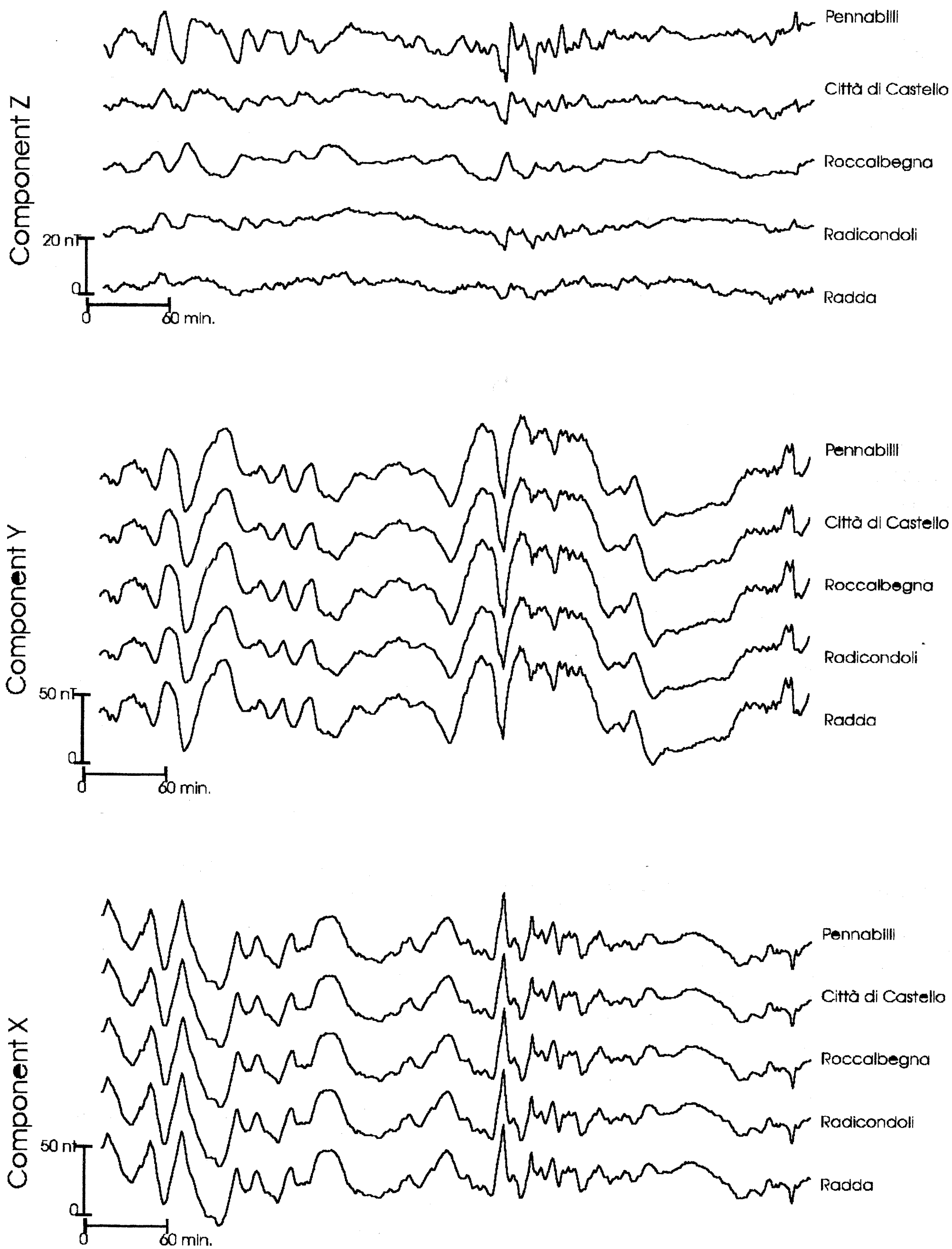

Fig. 2. Time domain representation of the bay-like event of May 7, 1992.

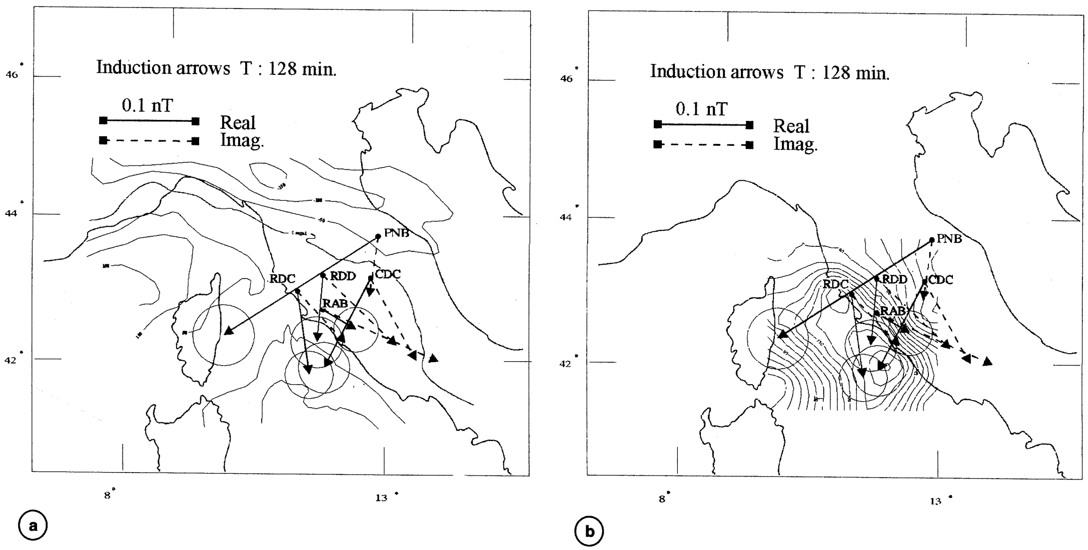

Fig. 3a,b. Induction arrows at $T = 128$ min, compared with: a) the gravimetric Bouguer anomalies; b) heat flow density (HFD) values (gravimetric anomalies: from Morelli and Nicolich, 1990; heat flow density (HFD) in mW * m^{-2}: from Mongelli *et al.*, 1989).

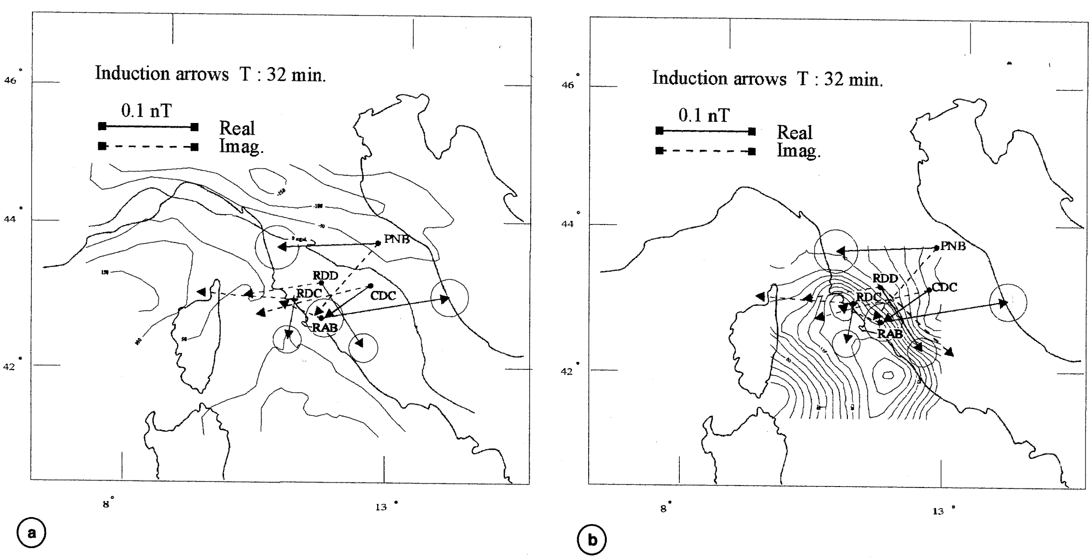

Fig. 4a,b. Induction arrows at $T = 32$ min compared with: a) the gravimetric Bouguer anomalies; b) heat flow density (HFD) values.

near the zero line of the gravimetric Bouguer anomaly. At RAB the vector points in a more eastward direction. The behaviour of RAB is also strongly confirmed by the arrows at the period $T = 32$ min. At CDC, RDD and RDC the vectors are directed SSW (fig. 4a,b), but the intensity of these vectors is smaller.

Figure 5 shows a significant difference between the RAB and the CDC real arrow's direction. The real arrow of CDC shows a clockwise (about 180°) rotation from lower to higher periods.

The maps (fig. 6a,b) of the hypothetical event for both east-west (EW) and north-south (NS) polarization suggest that, at the period of 128 min, there is a concentration of induced currents, perhaps due to a flexure of the conductive layer. At smaller periods the pattern of gradient shows two maxima respectively in the area of RAB and RDD.

Figure 7 shows two pseudosections AA′ and BB′ respectively striking E-W and N-S. The pseudosection AA′ also includes the data of two magnetovariational stations in Corsica, *i.e.* Asco and Campana (Cerv *et al.*, 1993), whose geographical coordinates are reported in the lower part of table I.

The AA′ pseudosection suggests the existence of a rather shallow zone with high electrical conductivity, which extends from Corsica to Tuscany. Proceeding eastwards from RDD, *i.e.* towards the Adriatic stations of PNB, CDC, and RDD the electrical conductivity decreases both laterally and vertically. The BB′ pseudosection, along a profile parallel to the coast, near the border of the flexure appearing in the AA′ pseudosection, emphasises the patterns of the electrical conductivity transverse to the deepening of the conductive layer shown by AA′. Within an area of enhanced electrical conductivity two maxima are located respectively at the north and at the south of the profile. The RAB station shows an anomalous electrical conductivity.

4. Discussion

From the above analysis, globally it appears that the deep electrical conductivity in Central

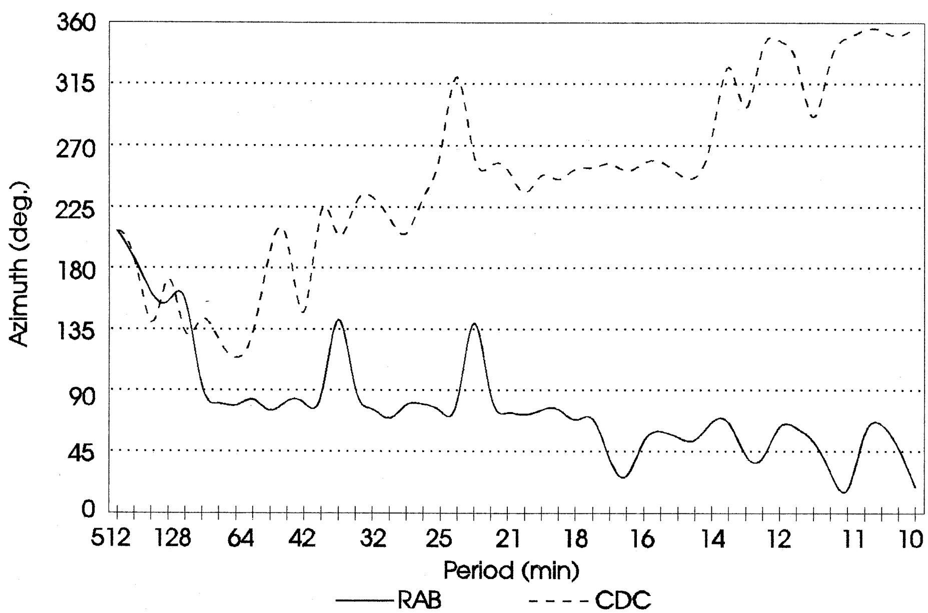

Fig. 5. Comparison between the azimuth of induction arrow at RAB and CDC, for different periods.

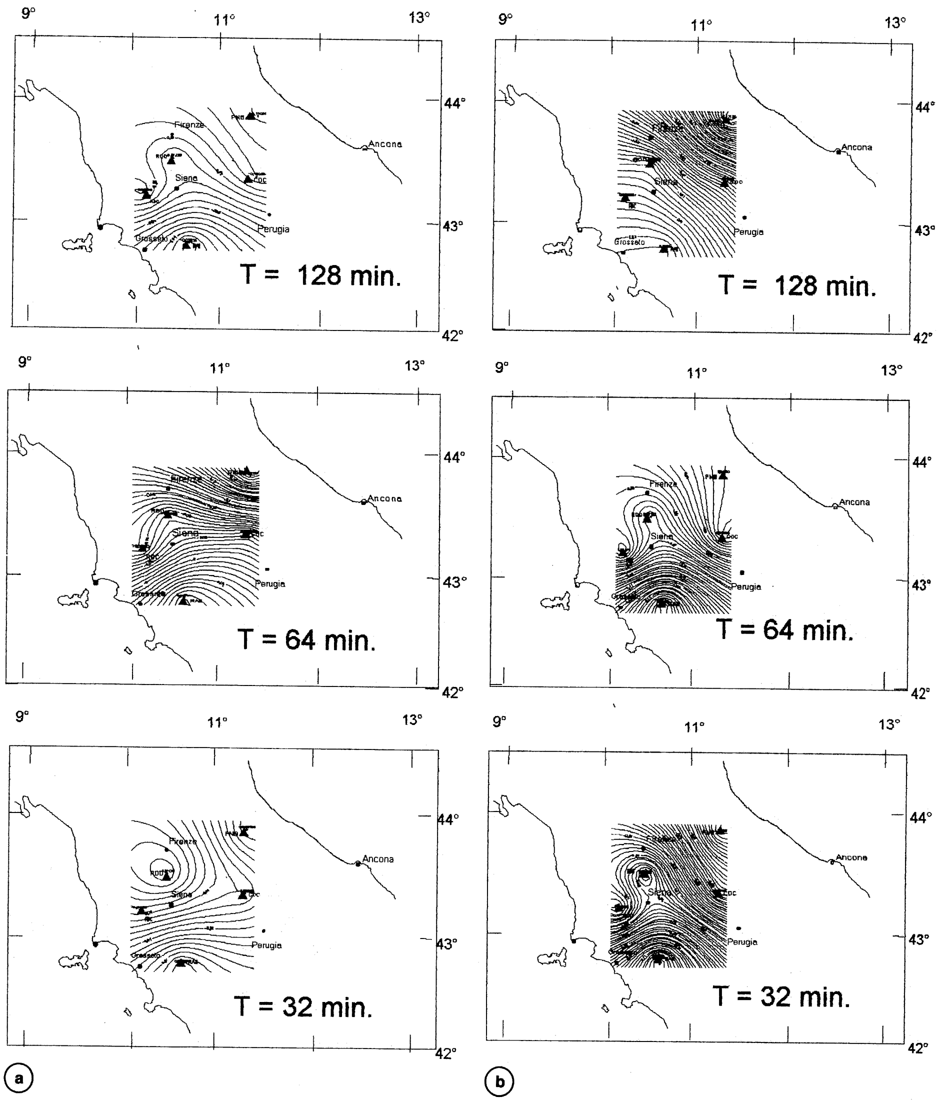

Fig. 6a,b. Maps of hypothetical events: a) for the east-west polarization; b) for the north-south polarization, at periods $T = 128$, 64 and 32 min (real component).

Italy is rather anomalous. As known, different crustal types occur in the area and the characteristics of the conductive subcrustal layers seem to indicate the existence of at least two different domains. The latter, as shown in figs. 6a,b and 7, are located respectively on the Tyrrhenian and Adriatic sides of the Apenninic chain. The different crustal types in the Tyrrhenian, Apenninic and Adriatic zone could be related to a marked chemical and physical activity of the underlying mantle (*e.g.* Morelli and Nicolich, 1990). Such activity of the mantle corresponds to an increase in electrical conductivity, emphasized by the behaviour of the

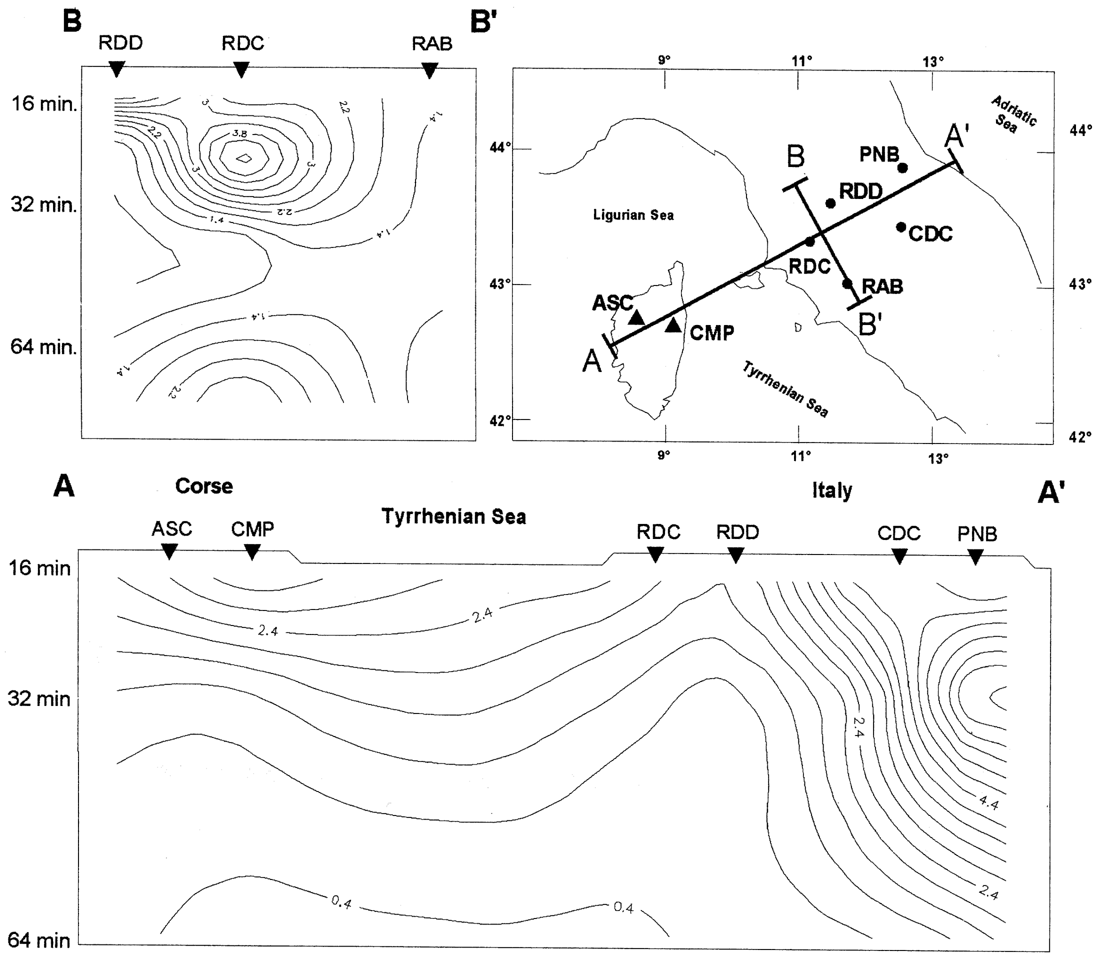

Fig. 7. Pseudosection $|Z/H|$; AA′: Corsica and Tuscany for the north-south polarization. Pseudosection $|Z/H|$; BB′ for the stations RDD, RDC, RAB with east-weat polarization.

Tyrrhenian stations (RDC,RDD,CDC) and by the almost steady directions of induction arrows at the Adriatic station (PNB). Conversely the site of RAB seems to be affected by other conductive bodies.

The pseudosections of fig. 7 seem to suggest the existence of a common feature of the layer, responsible for the magnetovariational results in Corsica and over the Tyrrhenian coast.

Both from time series analysis and transfer function representations it can be pointed out how the HFD anomaly constraints the response of «Tyrrenian» stations (RDC, RDD, CDC). This influence does not seem to decrease with period. Such behaviour could perhaps be ascribed to the effect of conductive structures playing a greater role, more developed in depth.

REFERENCES

BALIA, R., E. BOZZO, A. DE SANTIS, A. ELENA, G. GHEZZI, A. MELONI and G. RANIERI (1991): A magnetovariational study in Sardinia, *Phys. Earth Planet. Inter.*, **66**, 92-100.

CERV, V., E. BOZZO, A. DE SANTIS, A. ELENA, M. GAMBETTA, A. MARIOTTI, A. MELONI and J. PEK (1993): Electrical conductivity investigations of the Piedmont to Sardinia (Italy), *Phys. Earth Planet. Inter.*, **80**, 169-189.

CHAVE, A.D. and J.R. BOOKER (1987): Electromagnetic induction studies, *Rev. Geophys.*, **25**, 989-1003.

DELLA VEDOVA, B., I. MARSON, G.F. PANZA and P. SUHADOLC (1991): Upper mantle properties of the Tuscan-Tyrrhenian area: a framework for its recent tectonic evolution, *Tectonophysics*, **195**, 311-318.

EVERETT, J.E. and R.D. HYNDMAN (1967): Geomagnetic variations and electrical conductivity structure in South-Western Australia, *Phys. Earth Planet. Inter.*, **1**, 24-34.

GOUGH, D. I. (1989): Magnetometer array studies, Earth structure, and tectonic processes, *Rev. Geophys.*, **27**, 141-157.

GOUGH, D. I. and M.R. INGHAM (1983): Interpretation methods for magnetometer arrays, *Rev. Geophys. Space Phys.*, **21** (4), 805-827.

INGHAM, M.R., D.K. BINGHAM and D. I. GOUGH (1983): A magnetovariational study of a geothermal anomaly, *Geophys. J.R. Astron. Soc.*, **72**, 597-618.

LAVECCHIA, G. (1988): The Tyrrhenian-Apennines system: structural setting and seismotectogenesis, *Tectonophysics*, **147**, 263-296.

MONGELLI, F., G. ZITO, N. CIARANFI and P. PIERI (1989): Interpretation of heat flow density of the Apennine chain, Italy, *Tectonophysics*, **164**, 267-280.

MORELLI, C. and R. NICOLICH (1990): A cross section of the lithosphere along the European geotraverse southern segment (from the Alps to Tunisia), *Tectonophysics*, **176**, 229-243.